

This work was written as part of one of the author's official duties as an Employee of the United States Government and is therefore a work of the United States Government. In accordance with 17 U.S.C. 105, no copyright protection is available for such works under U.S. Law. Access to this work was provided by the University of Maryland, Baltimore County (UMBC) ScholarWorks@UMBC digital repository on the Maryland Shared Open Access (MD-SOAR) platform.

Please provide feedback

Please support the ScholarWorks@UMBC repository by emailing [scholarworks-group@umbc.edu](mailto:scholarworks-group@umbc.edu) and telling us what having access to this work means to you and why it's important to you. Thank you.

## Exterior and interior polar cusps: Observations from Hawkeye

S.-H. Chen,<sup>1,2,3</sup> S. A. Boardsen,<sup>2,3</sup> S. F. Fung,<sup>2,4</sup> J. L. Green,<sup>4</sup> R. L. Kessel,<sup>4</sup>  
L. C. Tan,<sup>2,3</sup> T. E. Eastman,<sup>5</sup> and J. D. Craven<sup>6</sup>

**Abstract.** Hawkeye plasma, magnetic field, and plasma wave instruments directly sampled the throat of the northern polar cusp as the orientation of the interplanetary magnetic field (IMF) changed from southward to northward on July 3, 1974. Two distinct regions in the polar cusp were identified based on magnetic field, plasma flow and magnetic and electric noise: the interior and exterior cusps. The observations show highly variable flows in the exterior portion of the cusp and constantly strong dawn-dusk flows in the interior portion during periods of strong IMF  $B_y$  component. Results of a minimum variance analysis of the magnetic field at each cusp interface crossing provides evidence that the magnetopause surface normal deviated highly from empirical models. During intervals of relatively steady solar wind dynamic pressure, the motion of the cusp relative to the slow moving spacecraft was modulated by the varying IMF clock angle as observed by IMP 8 in the upstream solar wind. The motion did not show a correlation with internal processes monitored by the  $AE$  index. We propose that observed plasma flow patterns and cusp motion are results of reconnection between the IMF and the magnetospheric magnetic field. Flow velocity observed in the interior cusp is consistent with stress balance for a reconnection process. This unique interval provides an opportunity for detailed studies of the plasma, magnetic field, and plasma wave properties in both the exterior and interior cusp.

### Introduction

The Earth's polar cusps are generally considered to be regions in which the heated solar wind plasma of the magnetosheath has direct access to the inner magnetosphere. Such penetrations of sheath plasma have been observed by spacecraft in the high-, middle- or low-altitude cusps for over 20 years [e.g., Heikkila and Winningham, 1971; Frank, 1971; Russell et al., 1971; Reiff et al., 1977, 1980; Burch et al., 1982]. As a result, two transition or boundary regions have been identified between the magnetosheath and the magnetosphere and shown to extend either equatorward or tailward from the cusps: (1) the entry layer sunward of the cusp [Haerendel and Paschmann, 1975; Paschmann et al., 1976] and (2) the plasma mantle extending tailward above the magnetotail lobe [Rosenbauer et al., 1975]. Several mechanisms have been proposed for the plasma entry processes that lead to the formation of these transition layers: reconnection between the interplanetary and magnetospheric magnetic fields [e.g., Dungey, 1968; Frank, 1971; Vasyliunas, 1972; Rosenbauer et al., 1975], diffusion of

particles across the magnetopause [e.g., Axford, 1970; Heikkila and Winningham, 1971] (see Reiff et al. [1977] for the discussion in detail), turbulent eddy convection [Haerendel et al., 1978], or impulsive penetration [Lemaire and Roth, 1978].

Of these the reconnection process has a pronounced effect on the cusp. Not only does reconnection provide a way to bring the solar wind particles into the magnetosphere, but it also controls the cusp's shape, size, and position [e.g., Potemra, 1992]. No matter where the reconnection process occurs on the magnetopause, the reconnected flux tube has to pass through either the northern or southern cusp region. The dominant factor that determines the initial location of reconnection and evolution of the reconnected flux tube is the orientation of the IMF [Crooker, 1979]. It has been shown that when the IMF is southward, reconnection occurs near the subsolar region [Dungey, 1968; Paschmann et al., 1979], and therefore the newly reconnected flux tube passes through the entry layer equatorward of the cusps. When the IMF is northward, the process occurs along the high-latitude magnetopause [Dungey, 1968; Kessel et al., 1996] and the newly reconnected flux tubes goes through the plasma mantle tailward of the cusps. When the IMF is east-west oriented and is positive (negative) the process occurs at the region duskside (dawnside) of the northern cusp [Gosling et al., 1991] and the newly reconnected flux tubes go through the plasma mantle, the entry layer, or mixture of the two. Using an OGO 5 cusp event, Kivelson et al. [1973] showed how the cusp position changes when the IMF turns from north to south. The general variability in the orientation of the IMF makes the situation more complex.

Studies of cusp dynamics have looked not only at the orientation of the IMF but also at the external solar wind dynamic pressure and internal dynamics as measured by the  $Dst$  and  $AE$  indices [Sandholt et al., 1983; Meng, 1983; Eather, 1985, and

<sup>1</sup>National Research Council, National Academy of Science, Washington, D. C.

<sup>2</sup>Space Physics Data Facility, NASA Goddard Space Flight Center, Greenbelt, Maryland.

<sup>3</sup>Now at Hughes STX Corporation, Greenbelt, Maryland.

<sup>4</sup>Space Science Data Operations Office, NASA Goddard Space Flight Center, Greenbelt, Maryland.

<sup>5</sup>Institute for Physical Science and Technology, University of Maryland, College Park.

<sup>6</sup>Geophysical Institute and Department of Physics, University of Alaska, Fairbanks.

Copyright 1997 by the American Geophysical Union.

Paper number 97JA00743.  
0148-0227/97/97JA-00743\$09.00

references therein]. *Sandholt et al.* [1983] concluded that there is a correlation between the sign and magnitude of IMF  $B_z$  and the dayside auroral location. *Meng* [1983] suggested that the equatorward shift of the cusp position is highly correlated with increasing magnitudes of southward IMF and the *Dst* index, but less correlated with the North American specific *AE* index. However, *Eather* [1985] showed that cusp motion was controlled mainly by the *AE* index as derived from the full set of stations and that IMF  $B_z$  had little effect. Accordingly, *Eather* [1985] concluded that the position of the dayside cusp is largely driven by substorm processes internal to the magnetosphere rather than by direct merging and erosion processes with the IMF. The controversy centered mainly on how validity of using ISEE 3 measurements as the near-Earth IMF  $B_z$ , or more strictly, the near-magnetopause sheath  $B_z$ . ISEE 3 was located  $\sim 220 R_E$  upstream of the bowshock. A simple estimate of the time shift of magnetic signatures from the position of ISEE 3 to the reconnection site on the magnetopause, based on the linear relationship between the mean solar wind flow velocity and displacement in  $X_{GSM}$ , were often inapplicable [*Crooker et al.*, 1982]. Using Dynamics Explorer data, *Burch et al.* [1985] demonstrated the *By* dependence of the plasma flow and the associated Birkland currents within the low-altitude polar region. Using measurements from the ISEE 2 fast plasma experiment, *Phillips et al.* [1993, and references therein] use a time-of-flight analysis to show the dispersive nature of the ion population exiting from the polar cusp when the IMF is southward and predict the source of ion injection. Although many mechanisms have been proposed to explain spatial or time variations of the cusps, we emphasize the reconnection process in this study because we observe cusp motion that is clearly modulated by the variation of the orientation of the IMF, and, also, because it provides a more direct explanation for observed plasma flow characteristics.

In this study, we make use of multiple cusp-magnetosheath crossings by the Hawkeye spacecraft and its observations of the magnetic field, plasma flow and plasma waves to study the geometry of the cusp, the magnetic reconnection process near the cusp, and the dynamics of the cusp in response to variations in IMF orientation during a period of steady solar wind dynamic pressure. On the basis of observations from IMP 8 in the upstream solar wind, the IMF during this event was directed mainly from dawn to dusk, but was slowly turning from south-to-north with numerous fluctuations in the  $B_z$  component. This allows us to study the cusp's motion, its plasma and field characteristics and, hence, the reconnection process at varying sites on the magnetopause. Because the *By* component was positive during the event, a high magnetic shear is expected at the magnetopause duskward of the northern cusp, where Hawkeye entered the magnetosphere. Plasma measurements show an anomalous flow direction that can be related to a reconnection process occurring on the magnetopause at the duskside of the cusp. We will describe first the orbit of Hawkeye, then the magnetic field, plasma, and plasma wave observations, the geometry of the cusp, and the reconnection process. The physical implications of these observations will then be discussed.

## Instrumentation

The Hawkeye spacecraft collected data from June 3, 1974, until April 28, 1978, supplying nearly four years of continuous data coverage. Hawkeye flew in a polar orbit ( $\sim 90^\circ$  inclination)

with an apogee of  $\sim 21R_E$  (geocentric) and a period of 51.3 hours. The Hawkeye onboard instruments included a triaxial fluxgate magnetometer, a VLF wave receiver, and a low-energy proton electron differential energy analyzer (LEPEDEA).

LEPEDEA had an  $8^\circ$  by  $30^\circ$  rectangular field of view, the center of which was oriented perpendicular to the spacecraft's spin axis. For each full rotation of the spacecraft ( $\sim 11$  s), this field of view swept out an area of angular dimension  $30^\circ$  by  $360^\circ$  on the celestial sphere. Both the plasma electron and proton channels were sampled in 16 logarithmically spaced energy pass bands (0.09 s duration per sample) as the analyzer potential ramped downward for energy coverage from  $\sim 45$  keV to 110 eV. The full energy sweep took 1.44 s and was obtained once every 11.52 s with sampling alternating between electrons and protons. Since the spacecraft spin period was approximately 11 s, each energy sweep was slightly offset in angular direction from the previous one such that a full two-dimensional energy-angle distribution in eight sectors was obtained for each particle species in approximately 3.5 min. For the event in this study, the spin axis was close to the Sun-Earth line, so the instrument sampled particle populations flowing mainly in the Y-Z (dawn-dusk) plane. The configuration is suitable for studies of dawn-dusk plasma flows.

The Hawkeye magnetometer was a triaxial fluxgate system with four automatic range setting: 150, 450, 1500, and 25000 nT. At the time the observations were made, the range setting was 150 nT (i.e. at the highest amplitude resolution for all three components). The time resolution was  $\sim 1.89$  s.

The VLF plasma wave receiver made 16 logarithmically spaced electric field measurements in the frequency range of 1.8 Hz to 178 kHz, and 8 magnetic field measurements in the frequency range of 1.8 Hz to 5.6 kHz. Approximately 22 s was needed to sample the entire frequency range. More detailed information on the spacecraft, its orbit and all instrumentation is provided by *Gurnett and Frank* [1977, 1978] and the appendices of *Farrell and Van Allen* [1990].

## Observation and Analysis

Figure 1a shows the projection of Hawkeye's trajectory in the  $X - Z_{GSM}$  plane for July 3, 1974 (day 184), along with the model magnetopause positions at  $Y_{GSM} = 0$  given by *Sibeck et al.* [1991] (the solid curve) and *Farris et al.* [1991] (the dashed curve) for the upstream solar wind condition at the time of crossing. Magnetic field line traces (the thin curves) in the noon-midnight meridian are also shown using the Tsyganenko 89 (T89) [*Tsyganenko*, 1989] model, with  $Kp = 2$  representing the state of the magnetospheric activity at the time of observation to indicate a possible cusp location. Note that the 3-hour resolution  $Kp$  index values were 2, 2<sup>-</sup>, 2<sup>-</sup>, and 3 at the times centered at 1330, 1630, 1930, and 2230 UT, respectively. We have chosen  $Kp = 2$  as the "average" state of the magnetospheric activity for the T89 model. Figure 1b shows the projection of the same orbit in the  $Y - Z_{GSM}$  plane. The magnetic field line traces of the T89 model (the thin curves diverge away from the center of the plot) originate from a circle  $3^\circ$  in diameter around the magnetic pole of the T89 model at the Earth's surface. The field direction (not shown) is toward Earth. Because there is no cusp geometry implemented in the T89 model, the choice of a circle  $3^\circ$  in diameter around the magnetic pole is arbitrary but demonstrates the direction of magnetic field vectors around the pole of the outer magnetosphere. The size and shape of the cusp based on this field

model may deviate highly from the actual cusp geometry. It is more useful to specify orientation of the wall of the cusp at the times of magnetopause crossings by studying the surface normal vectors. This will be done herein.

The upstream solar wind plasma and interplanetary magnetic field (IMF) measurements from the IMP 8 spacecraft are shown in Figure 2 for the period of interest. The GSM position of the spacecraft is given with UT along the abscissa, where, for example, its position at 1730 UT is near  $(10, -33, -3) R_E$ . The figure shows, from top to bottom, the bulk flow velocity ( $V_b$ ) in km/s, the number density ( $N_p$ ) in  $\text{cm}^{-3}$ , the dynamic pressure ( $P_{\text{dyn}}$ ) in nPa, three components of magnetic field ( $B_x$ ,  $B_y$ ,  $B_z$ ) and the total field strength ( $|B|$ ) in nT. The solar wind dynamic pressure during the interval was relatively steady ( $1.5 \pm 0.5$  nPa), while the IMF was oriented mainly eastward before 1720 UT and then gradually turned to the north. The field strength, on the other hand, remained relatively steady. Fluctuations in the field strength were less than 2 nT. During the turning of the IMF between 1700 and 1800 UT, there were large amplitude fluctuations ( $>5$  nT peak to peak) in the Z component with periods of a few minutes.

The magnetic field magnitude and components (GSM coordinates) for Hawkeye (heavy traces) are shown in Figure 3 for a 4-hour period beginning at 1500 UT. In order to discuss the possible relationship between the IMF orientation and the cusp dynamics, the three components and total field strength of the IMF at the IMP 8 position (light traces) are also shown. No time shift was applied when making the plot (see below). The scales on the y axes for the IMP 8 (Hawkeye) field traces are to the right (left). Note that the amplitude scales used for IMP 8 field traces are 6 times smaller than those used for Hawkeye. The positions of IMP 8 and Hawkeye are shown in Figure 4. The major separation between the two spacecraft is in  $Y_{GSM}$  ( $\sim 35R_E$ ), while the difference in the  $X_{GSM}$  positions is relatively small ( $\sim 2R_E$ ). The IMF clock angle, which is defined as  $\theta_{\text{clock}} = \tan^{-1}(B_y/B_z)$ , is shown in the bottom panel of Figure 3:  $\theta_{\text{clock}} > 0$  indicates IMF  $B_y > 0$ ;  $|\theta_{\text{clock}}| < 90^\circ$  ( $>90^\circ$ ) indicates IMF  $B_z > 0$  ( $B_z < 0$ ); and  $\theta_{\text{clock}} = 0^\circ$  ( $180^\circ$ ) thus means that the IMF is northward (southward). During the period of 1700–1810 UT, while moving inbound from the magnetosheath (Figure 1), Hawkeye encountered several regions of field depression that could be identified as cusp currents in which the magnetic field direction changed predominately from east-west to north-south (see the shaded regions in Figure 3). The observation suggest that the currents are distributed in layered structures instead of filaments, since a similar current structure was observed as the spacecraft moved repeatedly across it [cf. Fairfield and Ness, 1972]. The magnetic field variations at Hawkeye, in the intervals between the shaded regions, are generally seen to have the characteristics of the high-latitude magnetosheath magnetic field; negative  $B_x$ , strongly positive  $B_y$  and variations in  $B_z$ . This is not true for the last three intervals (see below). All indications are that those regions (unshaded) are associated with the exterior cusp. The positive  $B_z$  of the last three intervals between the shaded regions is possibly due to the draping effect of the magnetosheath field against the wall of the cusp facing the dawnside. On the basis of the plasma and plasma wave signatures, and the similarity of the observed magnetic field configuration with that of the model field (T89) (Figures 1a and 1b), it is concluded that Hawkeye entered the magnetosphere after  $\sim 1807$  UT.

The time lag in the field signatures between Hawkeye and

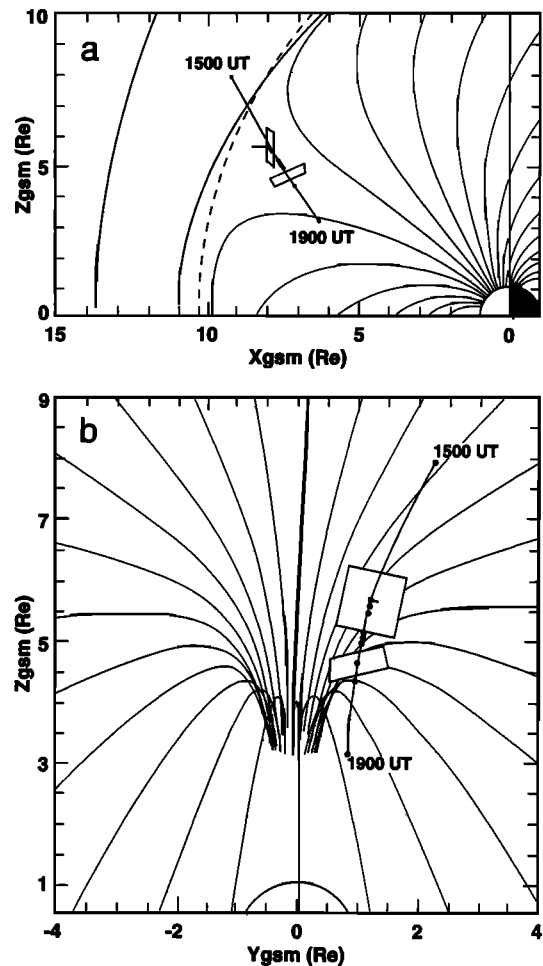


**Figure 1.** Projection of Hawkeye's trajectory in the (a)  $X - Z_{GSM}$  and (b)  $Y - Z_{GSM}$  plane, along with model magnetopause positions at  $Y_{GSM} = 0$  given by Sibeck *et al.* [1991] (the solid curve) and Farris *et al.* [1991] (the dashed curve). Magnetic field line traces (the thin curves) are also shown using the Tsyganenko 89 (T89) model for  $K_p = 2$  in the noon-midnight meridian to indicate a possible cusp location. The figure also identifies the tangential planes of the first and the last Hawkeye magnetopause crossings based on a minimum variance analysis of the magnetic field data. The magnetopause normal vectors in GSM coordinate for the first and the last crossings are  $(0.98, 0.20, -0.03)$  and  $(0.12, -0.33, 0.94)$ , respectively. The normal vector of the Sibeck *et al.* model magnetopause is  $(0.88, 0.11, 0.47)$ .

IMP 8 can be small due to the special orientation of IMF and relative position of the spacecraft. Figure 4 shows the projection of the average IMF between 1540 and 1750 UT onto the  $X - Y_{GSM}$  plane. The IMF makes an angle of  $\sim 63^\circ$  to the negative X axis. Considering the fact that the IMF is being slowed after its bowshock crossing and then draped against the magnetopause, the time lag between the magnetic field signatures observed at IMP 8 and Hawkeye becomes complex. On the basis of a gasdynamic model, the streamlines on the magnetopause have to go through the singular point at the nose of the magnetopause. In this case the time lag between the magnetic signature on a magnetic field line that intersect with a streamline on the magnetopause and the signature on the same field line but located in the upstream solar wind becomes infinity as the flow velocity at the singular point is zero. How-

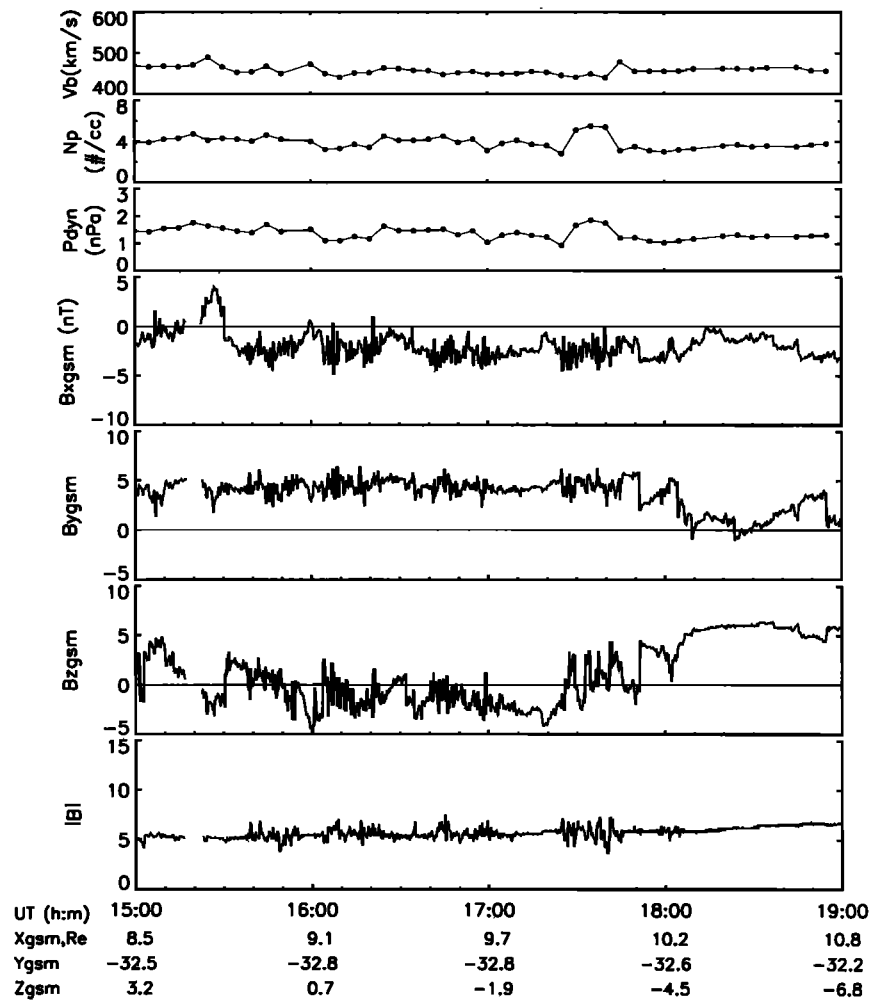


**Figure 2.** IMP 8 solar wind plasma and interplanetary magnetic field data in GSM coordinates on day 184, 1974. From top to bottom the panels display, the bulk flow velocity in kilometers per second, the number density in  $\text{cm}^{-3}$ , the dynamic pressure in nanopascals, three components of magnetic field, and the total field strength in nanoteslas.

ever, we can estimate the time lags by using (1) a simple schematic diagram that avoid the streamlines passing through the singular point and (2) a cross correlation between the field signatures observed at IMP 8 and Hawkeye. The time lag can be small if the IMF  $X$  component is negative and  $Y$  component is positive, as shown in Figure 4. Under this configuration the magnetic field signatures (field line labeled 1 in Figure 4) reach the nose of the bow shock before they reach the position of IMP 8. The field line of the part in the sheath travels at a speed slower but at a distance shorter than the part in the upstream solar wind before reaching the position of Hawkeye (the dashed curve in Figure 4). Accordingly, the time lag between the magnetic field signatures at IMP 8 and Hawkeye can be small if the signatures at Hawkeye were on a streamline that has some distance away from the magnetopause. During the interval of 1500–1600 UT, for example, the  $Z$  component field signatures at Hawkeye and IMP 8 (Figure 3) show a good correlation. The correlation becomes poorer as the draping effect of the IMF against the magnetopause becomes significant when Hawkeye approaches the magnetopause at 1650 UT, for example. Since there is a good correlation between the Hawkeye and IMP 8 magnetic field measurements in part of the time

interval, no time lag was applied to make Figure 3. Accordingly, the periods instead of phases of the magnetic fluctuations observed between IMP 8 and Hawkeye are more meaningful.

During the time when the field, plasma and wave measurements were made the spin axis of Hawkeye spacecraft made angles  $\sim 35^\circ$ ,  $72^\circ$  and  $119^\circ$  to the  $X_{GSM}$ ,  $Y_{GSM}$  and  $Z_{GSM}$  axes, respectively (Figure 5). The projections of the  $Y_{GSM}$  and  $Z_{GSM}$  axes onto the spin plane ( $Y'$  and  $Z'$  as shown in Figure 5) were nearly orthogonal ( $\sim 100^\circ$  separation). The angles  $Y'$ -to- $Y_{GSM}$  and  $Z'$ -to- $Z_{GSM}$  are  $18^\circ$  and  $29^\circ$ , respectively. Hence the observations of plasma flows in the spin plane would then provide reasonable estimates for the flows in the  $Y - Z_{GSM}$  plane. Six two-dimensional LEPEDA ion distribution functions in the spin plane are shown in Figure 6 for the intervals within the magnetosheath and the exterior cusp, as identified by the corresponding labels ( $a, b, \dots, f$ ) used in the bottom panel of Figure 3. The individual contours in each panel indicate constant phase space density, with the outer heavy line indicating  $10^7 \text{ s}^3/\text{km}^6$ . Four logarithmically spaced contours are drawn per decade, each of the same magnitude in every panel. The shadings for greater values of  $f(v)$  indicate that the local maxima in the distribution functions taken at different times.

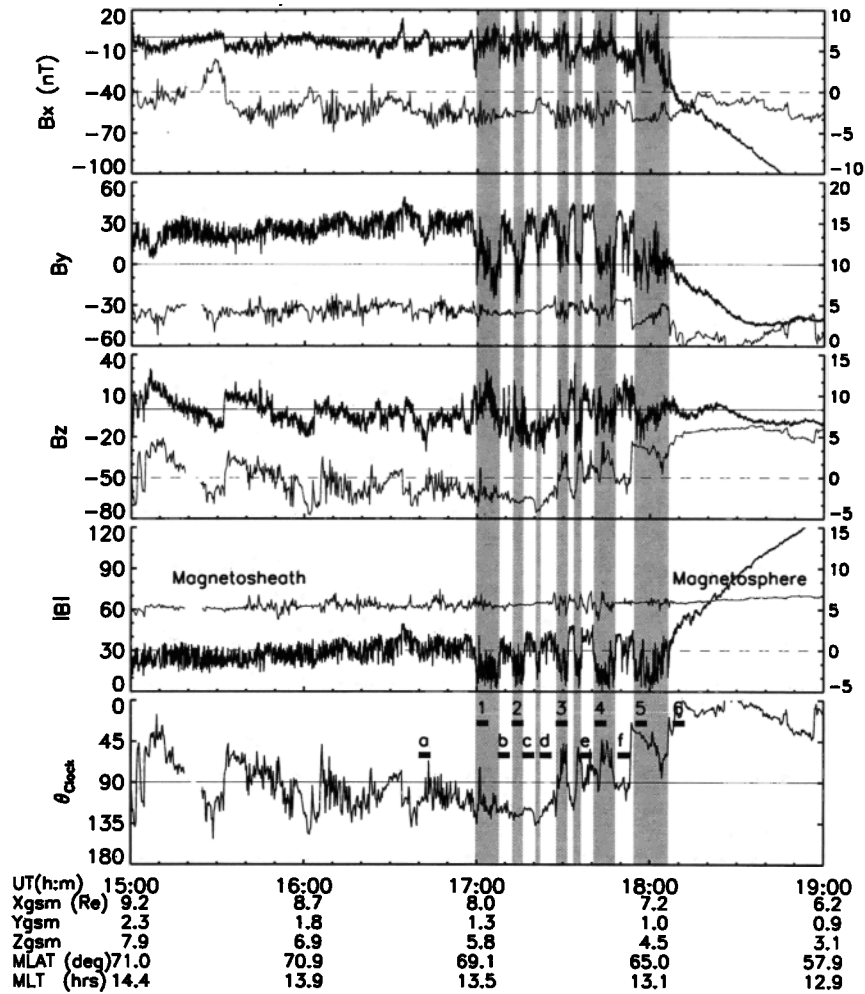


**Figure 3.** Magnetic field magnitude and three components (in GSM coordinates) measured by Hawkeye (dark curves) on day 184, 1974. Three components of the IMF from IMP 8 (the light curves) are also shown, but multiplied by a factor of 5 and shifted  $-40$  nT in magnitude (see Figure 2). The field magnitude is shifted by 20 nT instead  $-40$  nT. Since the difference in the  $X_{GSM}$  positions of IMP 8 and Hawkeye is small, no time lag is applied. The IMF clock angle  $\theta_{clock} = \tan^{-1}(B_Y/B_Z)$  is also shown in the bottom panel:  $\theta_{clock} > 0$  implies IMF  $B_Y > 0$ ;  $|\theta_{clock}| < 90^\circ$  ( $>90^\circ$ ) implies IMF  $B_Z > 0$  ( $B_Z < 0$ ); and  $\theta_{clock} = 0^\circ$  ( $180^\circ$ ) means that the IMF is northward (southward). The magnetosheath is to the left and the magnetosphere is to the right. The shaded regions indicated those intervals when Hawkeye was located within the interior cusp.

Projections of the local magnetic field vector onto the spin plane are also shown (the arrows). The radius of the outer most circular grid corresponds to a 50 nT field magnitude. The contours in Figure 6a show a typical sheath plasma flow in a direction  $\sim 45^\circ$  upward and duskward away from the noon-midnight plane, as expected for Hawkeye in the northern hemisphere and in the postnoon side (see Figure 1b). As Hawkeye moved down the throat of the cusp, the ion distribution functions varied with time in the exterior cusp (e.g., contours of Figure 6b and 6c), while the orientation of the magnetic field remained unchanged—dominated by the  $+Y$  component. The flower-shaped contours of Figures 6d, 6e, and 6f may result from rapid crossing of the spacecraft from one plasma region within the exterior cusp into another (also within the exterior cusp). Given the simplicity and limitations of the Hawkeye measurements, we only identify two major plasma regimes that have distinct characteristics: those of the exterior cusp and the interior cusp. The mean flow direction changes from mainly duskward in Figure 6a (to the right in the

figure) over the pole in the Figure 6b, dawnward (to the left) in Figure 6e and to slightly downward in Figure 6f. The distribution functions of Figures 6e and 6f are from regions that have the most typical characteristics of the exterior cusp, where the field and plasma are sheath-like but the flow pattern is controlled by the interaction between the magnetosheath and magnetospheric plasmas, for example, reconnection process and turbulence. Noticeably, the flow velocity for the majority of plasma in the exterior cusp (Figures 6e and 6f) is  $\sim 300$  km/s downward against the magnetosheath mean flow  $\sim 200$  km/s upward and slightly duskward (Figure 6a). The flow direction is close to field-aligned. This is consistent with flows coming from a reconnection site located at the duskside of the cusp.

Using the format of Figure 6, the ion distribution functions for the intervals of interior cusp (labeled 1–5) and the magnetospheric boundary layer—the cusp entry layer (labeled 6) are shown in Figure 7, using the same labeling scheme used in Figure 3. Flows in the interior cusp are mainly from dusk to dawn with changes from slightly poleward (north) to slightly

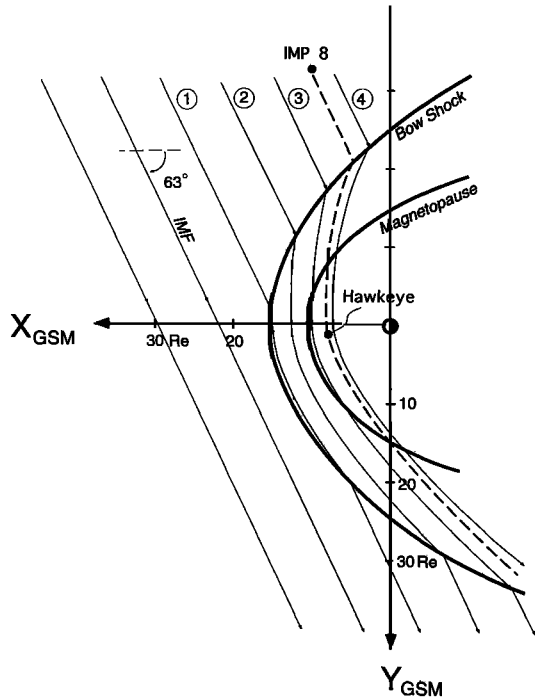


**Figure 4.** Diagram to illustrate the positions of IMP 8 and Hawkeye projected on to the  $X - Y_{GSM}$  plane, along with the projection of the average IMF between 1550 and 1750 UT. The thin curves with arrows represent the magnetic field projection in the plane. The IMF projection makes  $\sim 63^\circ$  with the negative  $X$  axis. The figure demonstrates the possible small time lag between the magnetic field signatures observed at IMP 8 and Hawkeye (dashed curve).

equatorward as the spacecraft moved deeper into the cusp. The flow speed also increased slightly from  $\sim 250$  to  $\sim 300$  km/s. The flow direction is similar to the one in the exterior cusp (Figures 6e and 6f). The magnetic field strength is weak on average and does not appear to have clear relationship with the flow direction. The last distribution function (panel 6) is from within the magnetosphere. According to the position and magnetic field configuration, the last contour plot quite possibly is the entry layer identified by *Haerendel and Paschmann [1975]* and *Paschmann et al. [1976]*. One of the properties of the entry layer is the presence of bidirectional ion streaming along the magnetic field. Panel 6 shows the similar characteristics as the one shown in the paper of *Paschmann et al. [1976]*.

The identification of cusp crossings based on enhancements in VLF-ELF magnetic noise has been used, for example, by *Scarf et al. [1972, 1974]*, *Van Allen et al. [1974]*, *Gurnett and Frank [1978]*, *Saflekos et al. [1979]*, and *Van Allen and Adnan [1992]*. We make use of this established association to check the validity of our preliminary cusp identification based on magnetometer measurements. A spectrogram of Hawkeye VLF-ELF magnetic and electric field fluctuations is shown in Plate 1 for the time interval of 1645–1815 UT. The white traces in both panels indicate the local electron gyrofrequency  $f_e$ . The enhancements in magnetic fluctuations on the lowest decade of the upper panel (few hertz to a few tens of hertz) occur when the electron gyrofrequency or the magnetic field strength is minimum (i.e., within the polar cusp). This is consistent with our identification of the cusp being located within the intervals of magnetic depression as well as within the funnel geometry of

the magnetopause (see Figure 1) based on the minimum variance analysis of magnetic field. The electric noise at frequencies above  $f_e$  was noticeably diminished at the magnetic depressions, for example, near 1705, 1745, and 1800 UT. Auroral kilometric radiation (AKR) ( $\sim 100$  kHz) was present at nearly all times between 1700 and 1840 UT. However, there were noticeable variations in the intensity of the AKR starting at  $\sim 1700$  UT. Its frequency spectrum is anti-correlated with the variation in the electron cyclotron frequency  $f_e$ . The variation in  $f_e$  reflects the changes in the position of Hawkeye relative to the cusp (i.e., cusp motion).

To compare the possible factors that drive the cusp motion externally and internally as suggested earlier [e.g., *Eather, 1985*], Hawkeye magnetic field data and the IMF clock angle from the bottom panels of Figure 3 are repeated (1645–1815 UT) in Figure 8 along with the  $AU$ ,  $AL$ , and  $AE$  indices for the same period. This figure shows the details of the variation of magnetic field strength measured by Hawkeye at 1.89-s time resolution, the 15-s resolution IMF clock angle, and the 2.5-min resolution (the highest available)  $AU$ ,  $AL$ , and  $AE$  indices during the multiple cusp entries. Although the time resolution of the indices is low compared with those for the other parameters, it is still sufficient to show the trend and the 5–10 min fluctuations in  $|B|$  and  $\theta_{clock}$ . Using the format of Figure 3, the magnetosheath is to the left and the magnetosphere is to the right. The shaded regions are identified as the interior cusp and the unshaded regions the exterior cusp. The labeled dark line segments define the intervals from which ion distribution functions are shown in this study. Rapid fluctuations of field strength (top panel) within both the exterior and interior cusp indicate that the measured plasma structures are much more complex than just single layers. These fluctuations may be caused by either temporal or spatial variations. The motion of the cusp as observed by Hawkeye is strongly modulated by the

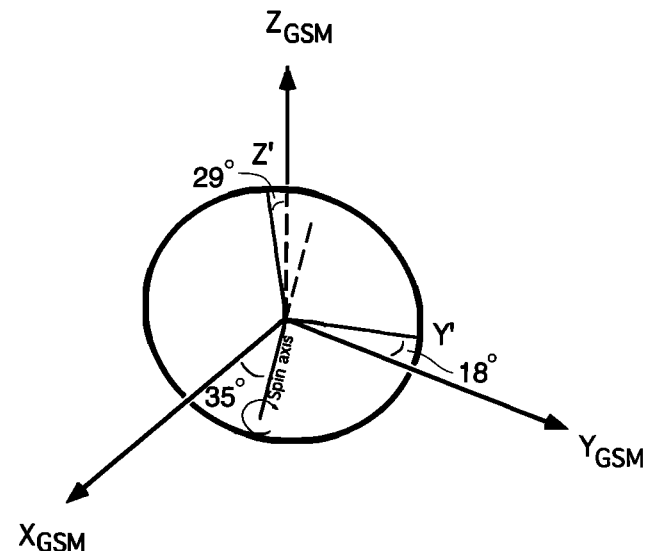


**Figure 5.** A schematic to illustrate the position of the Hawkeye spin plane relative to the GSM coordinate. The spin axis made a small angle ( $\sim 35^\circ$ ) to the  $X_{GSM}$  axis. Therefore, the spin plane was close to the  $Y - Z_{GSM}$  plane. The projections of the  $Y_{GSM}$  and  $Z_{GSM}$  axes on to the spin plane ( $Y'$  and  $Z'$  as shown) were nearly orthogonal to each other. The observations of plasma flows in the spin plane could provide reasonable estimates for the flows in the  $Y - Z_{GSM}$  plane.

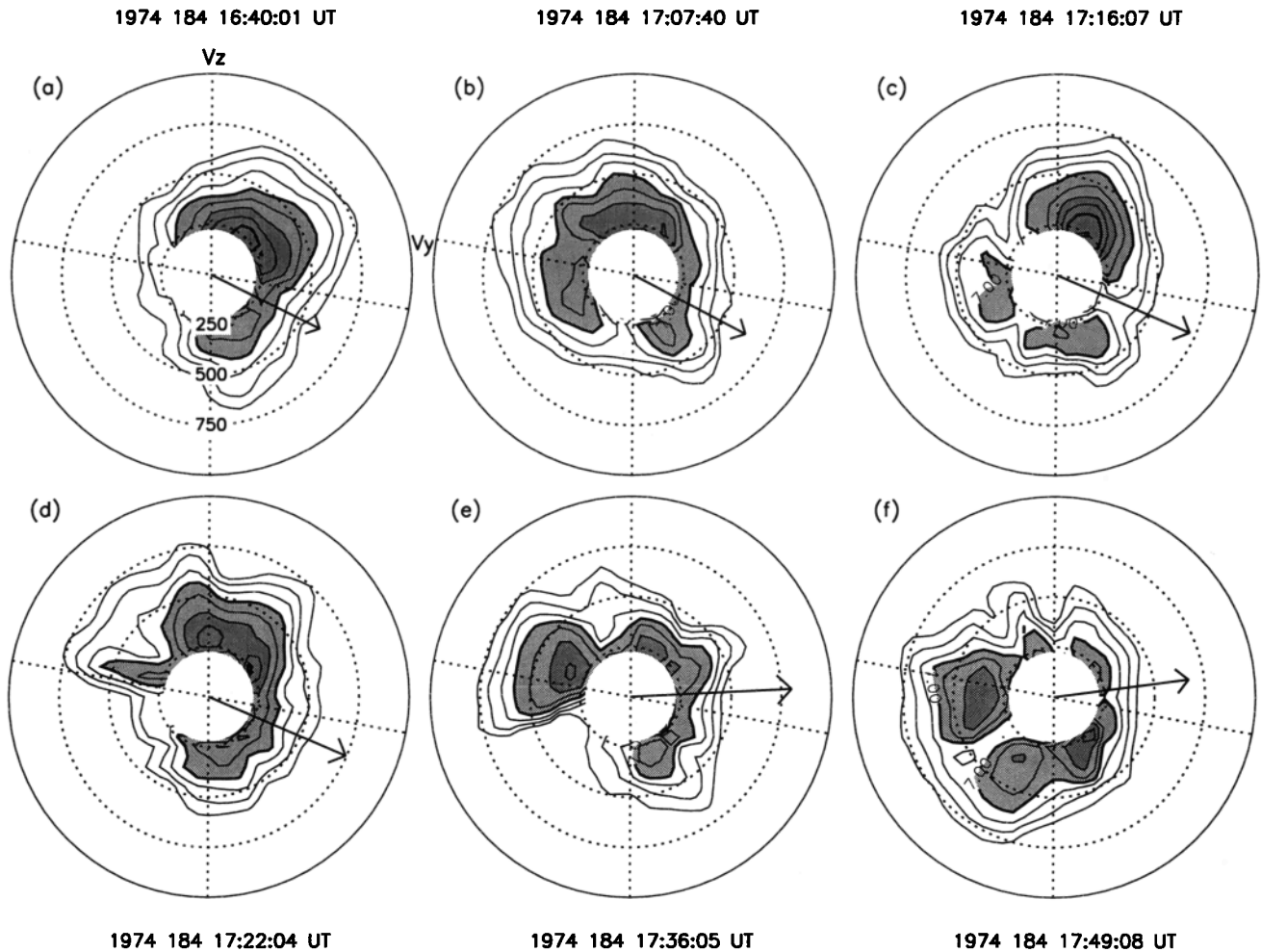


**Figure 6.** Two-dimensional LEPDEEA ion distribution functions in the spin plane for the intervals of exterior cusp. (a)–(f) Correspond to the labels used in the bottom panel of Figure 3. The individual contours in each panel indicate constant phase space density, with the outer heavy line at  $10^7$   $s^3/km^6$ . There are four logarithmically spaced contours per decade. The contour levels used in every panel are all the same. The shadings aids in the comparison among distribution functions taken at different times. The magnetic field projections onto the spin plane are also shown (the arrows). The radius of the outer most circular grid corresponds to 50 nT in field magnitude.

variations of the IMF clock angle  $\theta_{clock}$ . The  $AU$ ,  $AL$ , or  $AE$  index, however, shows less correlation, even when the IMF  $B_z$  changes from negative ( $\theta_{clock} < 90$ ) to positive ( $\theta_{clock} > 90$ ). This does not support the finding of *Eather* [1985] in which the equatorward (poleward) motion of the position of the cusp corresponds to increases (decreases) in the  $AE$  index.

The shape of the cusp surface is estimated through a minimum variance analysis on the magnetic field measurements at the times of cusp crossings. This analysis yields the eigenvalues  $\lambda$  and eigenvectors  $n_i$  of the linear system [cf. *Sonnerup and Cahill*, 1967; *Siscoe et al.*, 1968; *McPherron et al.*, 1972]

$$\sum_i (T_{ij} - \lambda \delta_{ij}) n_i = 0, \quad (1)$$

where  $\delta_{ij}$  is the Kronecker delta and the covariance matrix  $T_{ij}$  is given by

$$T_{ij} = \frac{1}{N} \sum_{k=1}^N (B_i^k - \bar{B}_i)(B_j^k - \bar{B}_j), \quad (2)$$

where the  $\bar{B}_l = (1/N) \sum_{m=1}^N B_l^m$  are averages of the pair of magnetic field components  $l = i$  and  $j$  selected from the three components  $x, y, z$ . Each of the six averages is taken using the  $N$  three-component measurements of  $\mathbf{B}$ . The data points in each variance analysis are chosen such that the magnetic field signatures best represent the plasma regions on both sides of the cusp boundary and the numbers of data points are roughly equal. For the sake of simplicity of presentation, we only plot the tangential planes to the surface for the first and the last magnetopause crossings that have significant eigenvalue ratios ( $\lambda_2/\lambda_3 \geq 2.5$ ) (Figure 1). The choice of the significant eigenvalue ratio is based on the work of *Sonnerup and Cahill* [1967] and *Lepping and Behannon* [1980]. Results of the variance analyses are listed in Table 1 for all the cusp interface crossings. The cusp interface surface normal vectors (in GSM coordinates) are (0.98, 0.19, 0.02) and (0.39, -0.25, 0.88), respectively, for the first (No. 2 in Table 1) and the last (No. 11 in Table 1) crossings of well-defined normal vectors. The normal vector of the Sibeck model magnetopause is (0.88, 0.11, 0.47).

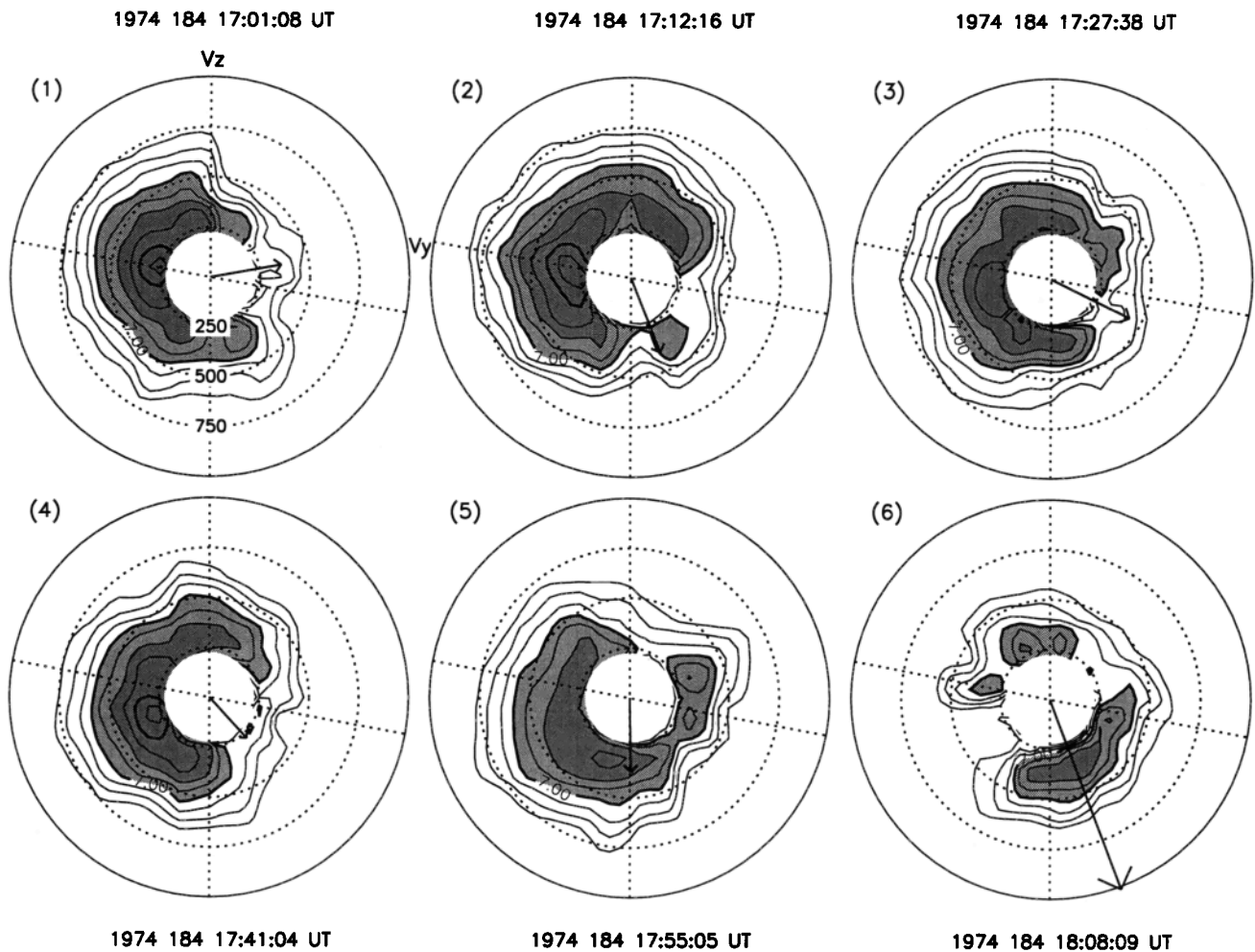


**Figure 7.** A repeat of Figure 6 but for the intervals of interior cusp (as labeled 1–5 in Figure 3) and the exterior cusp (as labeled 6 in Figure 3).

Most of the normal vectors labeled No. 1 to 10 have dominant  $X_{GSM}$  components and some of them have finite positive  $Y_{GSM}$  components. The positions of the cusp interface crossings ( $r$  in Table 1) highly deviates from the model magnetopause, which is  $\sim(9, 2, 6) R_E$  (Figure 1) at the same longitude and latitude and under the same solar wind conditions. Accordingly, the orientations of the magnetopause at the spacecraft crossings more nearly mimic the shape of the cusp.

### Discussion and Summary

By analyzing an interval on July 3, 1974, when Hawkeye repeatedly crossed different parts of the northern polar cusp, we are able to outline the structure of the exterior and interior regions of the polar cusp. We briefly summarize the plasma regimes seen by the Hawkeye spacecraft transiting through the cusp as the following. Hawkeye was inbound from the magnetosheath (label a in Figure 3) at the beginning of the interval and into the magnetosphere (label 6 in Figure 3 or 9) at the end. During its transit, it crossed the following regions: interior cusp (label 1 in Figure 3 or 9), exterior cusp (label b), interior cusp (label 2), exterior cusp (label c), exterior cusp (label d), interior cusp (label 3), exterior cusp with flows of reconnection (label e), interior cusp (label 4), exterior cusp with flows of reconnection (label f), interior cusp (label 5), and entry layer

(label 6). Figure 10 shows a schematic illustration of the plasma flow pattern and magnetic field geometry (in the cusp frame) that might have been observed by Hawkeye during the cusp entry. The top and bottom panels are for noon-midnight and dawn-dusk projections, respectively. The open (solid) circles represent the times of observation for ion distribution functions labeled a–f (1–6). Some labels are not shown for the sake of clarity. The light (dark) shaded area in the upper panel indicates exterior (interior) cusp. In the lower panel, the thick curve indicates the sheath magnetic field, and the open arrows represent plasma flows. In the exterior cusp, Hawkeye observed a relatively turbulent flow where flow direction is highly deviated from the magnetosheath mean flow (Figure 6). The magnetic field in the exterior cusp, however, remains sheath-like with a dominant  $Y$  component (Figures 3 and 8). In the interior cusp, the flow is more ordered. The flow direction is downward and slightly downward (Figure 7) as observed from the early afternoon hours of local time. The magnetospheric  $B_y$  is negative at the region duskside of the cusp and becomes dominant near 1800 MLT based on the  $\Psi 89$  field model. In contrast, the magnetosheath  $B_y$  is positive and is the dominant component ( $\theta \approx 90^\circ$ ) in the exterior cusp (Figure 3). Accordingly, there must be a region duskside of the cusp where the magnetic field in the magnetosheath and magnetosphere are

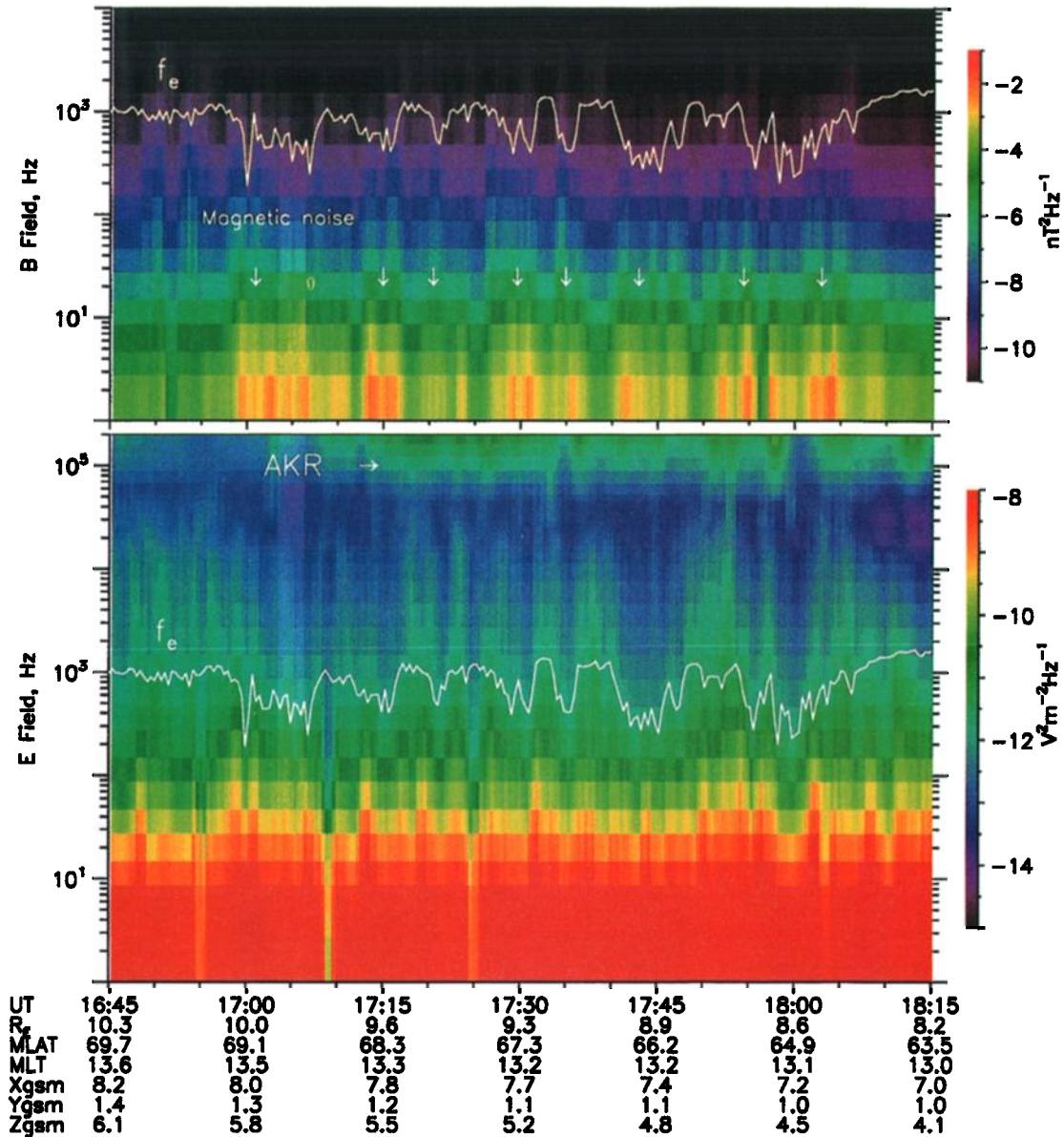


**Plate 1.** Hawkeye plasma wave frequency-time spectrogram of VLF-ELF magnetic and electric fields for day 184, July 3, 1974. The white traces in both panels indicate the electron gyrofrequency. The enhancements in magnetic fluctuations on the lowest decade of the upper panel (few hertz to a few tens of hertz) occur when the electron gyrofrequency or the magnetic field strength is minimum (indicating by white arrows, i.e., within the polar cusp). The electric noise at frequencies about  $f_e$  was noticeably diminished at the magnetic depressions, for example, near 1705, 1745, and 1800 UT. Auroral kilometric radiation (AKR) was present nearly all times between 1700 and 1840 UT.

antiparallel (Figure 9). This implies that reconnection may be occurring within a region duskward of the cusp when Hawkeye was in the cusp and observed the large-scale flow patterns.

If reconnection occurs, the magnetopause should be a rotational discontinuity [Sonnerup, 1974] and acquire a finite normal component ( $B_N$ ). Because of wave and instrumental noise or to inherent inaccuracies in calculating the boundary coordinate, it is difficult to establish the existence of the normal component  $B_N$ . Paschmann *et al.* [1990] suggest using plasma data to check for the existence of a moving frame of reference (de Hoffman-Teller frame or HT) in which plasma flow is aligned with  $B$ . If the flow is Alfvénic in the HT frame, then the

discontinuity is a rotational discontinuity. This is the so-called Walén relation ( $\mathbf{v} = \mathbf{v}_{HT} \pm \mathbf{B}/\sqrt{\mu_0\rho}$ ) based on tangential momentum balance, that predicts a linear relationship between the plasma velocity and the magnetic field. As a result of reconnection, reconnected field lines move with the de Hoffman-Teller speed  $V_{HT}$  along the magnetopause relative to the inertial frame [e.g., Cowley, 1982]. In this moving frame the incoming and outgoing flows are field aligned, and the convection electric field therefore vanishes. Because a kink in the field propagates along the field into the magnetosheath plasma at the Alfvén speed  $V_A$ , the incident magnetosheath flow speed in the HT frame is  $V_A$ , where  $V_A$  is calculated in the magne-

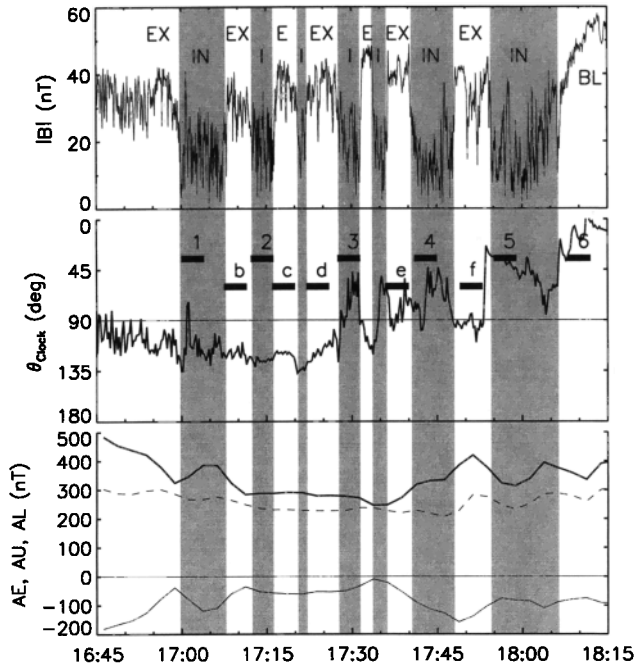


**Figure 8.** (top to bottom) The field strength observed by Hawkeye at 1.89-s time resolution, the 15-s IMF clock angle measured by IMP 8 and the 2.5-min resolution  $AU$  (the dashed curve),  $AL$  (the thin curve), and  $AE$  (the thick curve) indices. The shaded regions are intervals of interior cusp observation and the unshaded regions are for the exterior cusp. The labeled dark line segments in the middle panel are the intervals when ion distribution functions are shown in this paper.

tosheath adjacent to the magnetopause [e.g., *Sonnerup et al.*, 1990].

To check whether the flow in the interior cusp, the outflow region of reconnection, is consistent with a reconnection process, we estimated the flow velocity. We use the magnetic field in the exterior cusp, the inflow region, as the  $\mathbf{B}$  in the Walén relation. The flow velocity in the interior cusp in the  $Y-Z$  plane as measured by the two-dimensional LEPDEA instrument was  $\sim 300$  km/s in the spacecraft frame (Figure 7). Since Hawkeye did not measure the  $X$  component of the flow velocity, the total speed could be higher than 300 km/s. The local Alfvén speed  $V_{A1}$  in the exterior cusp, the inflow region of reconnection, was  $\sim 154$  km/s (using  $N_p = 5 \text{ cm}^{-3}$ ,  $|B| = 35$  nT). The spacecraft speed was only a few km/s and was ne-

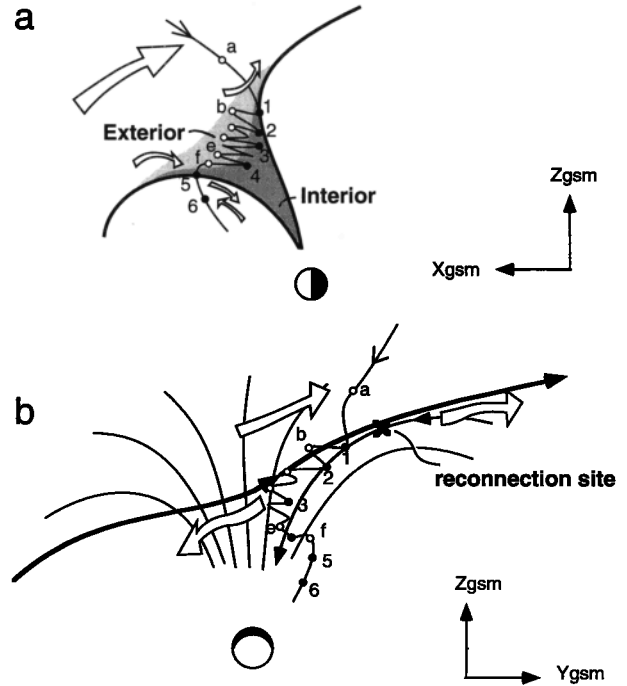


**Figure 9.** Schematic to illustrate the plasma flow pattern and magnetic field geometry in the cusp frame which might have been observed by Hawkeye during the cusp passage: (a) noon-midnight and (b) dawn-dusk projections. The open (solid) circles represent the times when ion distribution functions labeled a–f (1–6) were measured. Some labels are not shown for the sake of clarity. The light (dark) shaded area in the top panel indicates exterior (interior) cusp. In the bottom panel, the thick curve indicates the sheath magnetic field. The open arrows represent plasma flows.

glected. The flow speed of the outflowing plasma from a reconnection site was about  $2V_{A1}$  relative to the inertial frame fixed on the Earth. We also assumed that the reconnection site was moving in the direction of laminar flow in the sheath, mainly tailward and slightly duskward, at a speed  $V_{SH} = 250$  km/s comparable with the local sheath flow speed just outside the magnetopause. Figure 10a shows schematically the construction of the relevant flow vectors at the proposed reconnection site on the magnetopause: projections of flow vectors and the magnetosheath and magnetospheric magnetic fields in the plane tangent to the magnetopause at the reconnection site

**Table 1.** List of the Intervals and Results for Which the Minimum Variance Analysis Performed

No.	Time Intervals, UT	From-To	$r, R_E$	$(\lambda_1, \lambda_2, \lambda_3)$	$\lambda_2/\lambda_3$	$\hat{n}$ , GSM
1	1655:00–1705:00	EX-IN	(8.0, 1.3, 5.8)	(313, 67, 31)	2.2	? (0.87, 0.25, 0.42)
2	1704:00–1712:00	IN-EX	(7.9, 1.3, 5.6)	(331, 114, 29)	3.9	✓ (0.98, 0.19, 0.02)
3	1708:50–1715:58	EX-IN	(7.9, 1.2, 5.5)	(258, 130, 35)	3.7	✓ (0.95, 0.09, 0.29)
4	1713:02–1720:10	IN-EX	(7.8, 1.2, 5.4)	(363, 73, 36)	2.0	? (0.97, -0.02, 0.26)
5	1724:00–1731:00	EX-IN	(7.7, 1.1, 5.2)	(140, 44, 32)	1.4	? (0.84, 0.06, 0.54)
6	1730:22–1733:12	IN-EX	(7.6, 1.1, 5.1)	(355, 38, 17)	2.2	? (0.61, 0.61, -0.51)
7	1731:54–1735:52	EX-IN	(7.6, 1.1, 5.1)	(516, 69, 12)	5.8	✓ (0.88, 0.42, -0.21)
8	1734:16–1738:48	IN-EX	(7.6, 1.1, 5.0)	(433, 49, 10)	4.9	✓ (0.97, 0.24, -0.04)
9	1737:35–1744:17	EX-IN	(7.5, 1.1, 4.9)	(350, 63, 23)	2.7	✓ (0.98, 0.15, -0.14)
10	1746:09–1749:51	IN-EX	(7.4, 1.1, 4.8)	(646, 61, 15)	4.0	✓ (0.92, 0.30, -0.25)
11	1752:36–1756:18	EX-IN	(7.3, 1.0, 4.6)	(321, 108, 43)	2.5	✓ (0.39, -0.25, 0.88)
12	1800:04–1816:51	IN-BL	(7.1, 1.0, 4.4)	(358, 32, 14)	2.3	? (0.12, -0.33, 0.93)

the vector analysis is shown in Figure 10b. The de Hoffman-Teller speed  $V_{HT}$ , along the magnetopause relative to the inertial frame fixed on the Earth (the origin  $O$ ), is [cf. Cowley and Owen, 1989]

$$\mathbf{V}_{HT} = \mathbf{V}_{SH} - V_{A1} \hat{\mathbf{b}}_{SH} \quad (3)$$

The flow velocity  $\mathbf{V}_{BL}$  in the boundary layer of outflow region in the inertial frame (the origin  $O$ ) is given by

$$\begin{aligned} \mathbf{V}_{BL} &= V_{A2} \hat{\mathbf{b}}_{BL} + \mathbf{V}_{HT} \\ &= (V_{A2} \hat{\mathbf{b}}_{BL} - V_{A1} \hat{\mathbf{b}}_{SH}) + \mathbf{V}_{SH} \\ &\cong (V_{ySH} - 2V_{A1}) \hat{\mathbf{y}} + V_{xzSH} \hat{\mathbf{z}}, \end{aligned} \quad (4)$$

where we are assuming the Alfvén speed  $V_{A2}$  in the interior cusp is equal to  $V_{A1}$  in the exterior cusp. However, it is likely smaller and the direction of the magnetic field is opposite (anti-parallel merging). As the proposed reconnection site was at the postnoon side of the cusp, the  $y$  component of the sheath flow  $V_{ySH}$  was positive (flowing toward dusk) and magnitude was a fraction of 250 km/s, say 50 km/s. Therefore the flow speed in the boundary layer of outflow region in  $-\hat{\mathbf{y}}$  direction was  $< 2 V_{A1}$  ( $\sim 250$  km/s) in the rest frame of the Earth. Therefore the observed outflowing speed of plasma at the sunward/dawnward side of reconnection site in the Earth frame, which was 300 km/s, was comparable or greater than the theoretical estimate (the  $y$  component of  $\mathbf{V}_{BL}$ ). This is consistent with the criterion of flow speed in the outflow region of a reconnection site.

In this event, the motion of the cusp past Hawkeye appeared to be driven by an external process indicated by the IMF clock angle  $\theta_{clock}$  instead of an internal process indicated by the  $AU$ ,  $AL$  or  $AE$  index (Figures 3 and 8). Although the phases between the variation of the IMF clock angle and the motion of the cusp can hardly be predicted because of the ambiguity in the time shift between the magnetic signatures observed at IMP 8 and Hawkeye, the periods of the two somehow match well, particularly in the time interval 1715–1810 UT (Figure 8). The discrepancy between our result and *Eather's* [1985] may be due to the difference in the time scales that are used in the cross correlations. The correlation between the position of the cusp and the  $AE$  index obtained by *Eather* [1985] is good for a time scale of a couple hours while ours is good to minutes. The cusp then moved poleward after 1810 UT as the IMF turned steadily northward and the  $B_x$  component observed by Hawkeye turned gradually negative and became dominant. The negative  $X$  component is one of the field characteristics in the magnetosphere at a location equatorward of the northern cusp (Figure 1). The ion distribution function revealed bidirectional ion streaming along the field line (panel 6 in Figure 7). The characteristic of the bidirectional ion streaming is seen in the entry layer [Paschmann *et al.*, 1976]. A possible cause of the bidirectional ion streaming is reconnection at high latitudes. When the IMF turns northward, the reconnection site moves to a position poleward of the cusp [Kessel *et al.*, 1996]. The accelerated flows of the branch near the cusp may flow into lower latitudes along the reconnected field lines which have one of their ends tied to the Earth. The reconnected field lines then convect equatorward and formed the entry layer. While keeping the newly reconnected field lines feeding the entry layer and accelerated plasma flowing into low altitudes, the particles that have larger pitch angles are reflected before reaching the ionosphere. This may explain why the bidirec-

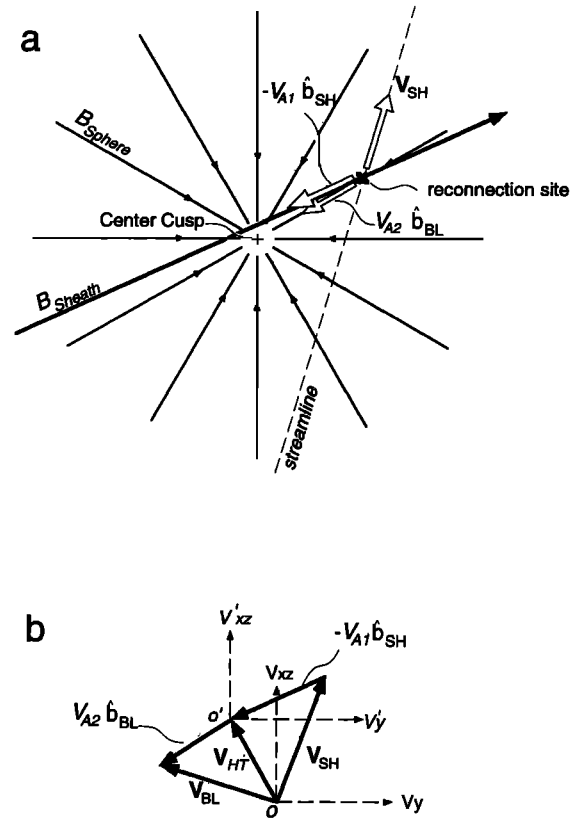


**Figure 10.** Schematic to illustrate the reconnection process. (a) The projection of magnetic fields and flow vectors in the plane tangent to the magnetopause at the reconnection site. The magnetic field of the magnetosphere and magnetosheath (as labeled) as denoted by solid lines with arrows and the open arrows denote the flows. The dashed line is a streamline passing through the reconnection site and the stagnation point (not shown) at the subsolar region. (b) The flow velocity  $\mathbf{V}_{BL}$  expected to be seen in the boundary layer of reconnection (the interior cusp) in a rest frame fixed on the Earth at  $O$ . Origin of the de Hoffman-Teller frame,  $O'$ , is also shown.

tional ion streaming along the field line was observed in the entry layer. The poleward movement of the cusp also implies that magnetic flux of the magnetosphere piled up at the dayside. Such piling-up can result from decreases in solar wind dynamic pressure or high latitude reconnection which brings magnetic fluxes from nightside to dayside over the magnetic poles. We prefer the latter option because the solar wind dynamic pressure showed essentially no change.

The shape of the cusp cannot be uniquely determined in this study since only one spacecraft made measurements of the cusp. However, we have estimated its shape by calculating boundary normal vectors using minimum variance analysis on magnetic field measurements at each cusp interface crossing. The magnetopause normal vectors in GSM coordinate for the first and the last crossings are (0.98, 0.19, 0.02) and (0.39, -0.25, 0.88), respectively. The normal vector of the Sibeck model magnetopause is (0.88, 0.11, 0.47). As shown in Figure 1, the planes tangent to the magnetopause or “the wall of the cusp” at the first and the last current layer crossings mimic a funnel shape. The positions of the magnetopause crossings deviate from the empirical models of *Sibeck et al.* [1991] and *Farris et al.* [1991] for which they used mainly low-latitude

magnetopause crossings. Similar cusp crossings using Hawkeye measurements at different parts of the cusp to picture the shape of the cusp in three-dimension under different solar wind conditions would be necessary to illustrate the three-dimensional shape.

In summary, we show the first clear and unambiguous in situ measurements of plasmas, magnetic fields, and plasma waves in the exterior and interior cusp and the cusp's response to the IMF. The exterior cusp is defined as the region of magnetosheath-like field and plasma flow controlled by the interaction between the magnetosheath and magnetospheric plasmas (i.e., reconnection process or turbulence). The interior cusp is the region of field depression, boundary layer plasma, stronger magnetic noise with weaker electric field noise than in the magnetosheath or inner magnetospheric boundaries. Results of a minimum variance analysis of the magnetic field during the intervals of cusp interface crossings provides strong evidence that the magnetopause normals can be highly deviated from the empirical models of *Sibeck et al.* [1991] and *Farris et al.* [1991]. While solar wind dynamic pressure was relatively steady, the cusp motion relative to the slow-moving spacecraft was modulated by the varying IMF clock angle as observed by IMP 8 in the upstream solar wind since no clear correlation with an internal process was found, as indicated by the *AE* index and proposed by *Eather* [1985]. To explain these results we propose that the anomalous flow pattern and the motion of the cusp are results of reconnection between the IMF and the magnetospheric magnetic field. The flow velocity in the interior cusp is consistent with the theoretical estimate of a reconnection process based on a stress balance calculation. This unique interval provides an excellent opportunity for detailed studies of the plasma, magnetic field, and plasma wave properties in the exterior and interior cusp.

**Acknowledgments.** We thank the NSSDC for supplying the Hawkeye and IMP-8 data. We thank J. Van Allen, A. Lazarus, and R. Lepping for making the Hawkeye, IMP 8 plasma and IMP 8 magnetic field data, respectively, available to NSSDC. The author S. H. C. thanks the support from the National Research Council Associateship Program, National Academy of Science. The research conducted at the Space Science Data Operations Office, Goddard Space Flight Center was performed under the auspices of the National Aeronautics and Space Administration. The work at the Hughes STX Corporation was performed under NASA grant NAS5-97059. The work at the University of Maryland was performed under NSF grant ATM-9411766. The work at the University of Alaska was funded by NASA grant NAGW-3441.

The Editor thanks E. A. Bering and another referee for their assistance in evaluating this paper.

## References

- Axford, W. I., On the origin of radiation belt and auroral primary ions, in *Particles and fields in the Magnetosphere*, edited by B. M. McCormac, p. 46, D. Reidel, Norwell, Mass., 1970.
- Burch, J. L., P. H. Reiff, R. A. Heelis, J. D. Winningham, W. B. Hanson, C. Gurgiolo, J. D. Menietti, R. A. Hoffman, and J. N. Barfield, Plasma injection and transport in the mid-altitude polar cusp, *Geophys. Res. Lett.*, **9**, 921, 1982.
- Burch, J. L., P. H. Reiff, J. D. Menietti, R. A. Heelis, W. B. Hanson, S. D. Shawhan, E. G. Shelley, M. Sugiura, D. R. Wiemer, and J. D. Winningham, IMF By-dependent plasma flow and birkeland currents in the dayside magnetosphere, 1, Dynamics explorer observations, *J. Geophys. Res.*, **90**, 1577, 1985.
- Cowley, S. W. H., The causes of convection in the Earth's magnetosphere: A review of developments during the IMS, *Rev. Geophys.*, **20**, 531, 1982.
- Cowley, S. W. H., and C. J. Owen, A simple illustrative model of open flux tube motion over the dayside magnetopause, *Planet Space Sci.*, **37**, 1461, 1989.
- Crooker, N. U., Dayside merging and cusp geometry, *J. Geophys. Res.*, **84**, 951, 1979.
- Crooker, N. U., G. L. Siscoe, C. T. Russell, and E. J. Smith, Factors controlling degree of correlation between ISEE 1 and ISEE 3 interplanetary magnetic field measurements, *J. Geophys. Res.*, **87**, 2224, 1982.
- Dungey, J. W., Waves and particles in the magnetosphere, in *Physics of the Magnetosphere*, edited by R. L. Carovillano, J. F. McClay, and H. R. Radoski, p. 246, D. Reidel, Norwell, Mass., 1968.
- Eather, R. H., Polar cusp dynamics, *J. Geophys. Res.*, **90**, 1569, 1985.
- Fairfield, D. H., and N. F. Ness, IMP 5 magnetic field measurements in the high-latitude outer magnetosphere near the noon meridian, *J. Geophys. Res.*, **77**, 611, 1972.
- Farrell, W. M., and J. A. Van Allen, Observations of the Earth's polar cleft at large radial distances with the Hawkeye 1 magnetometer, *J. Geophys. Res.*, **95**, 20,945, 1990.
- Farris, M. H., S. M. Petrinec, and C. T. Russell, The thickness of the magnetosheath: Constraints on the polytropic index, *Geophys. Res. Lett.*, **18**, 1821, 1991.
- Frank, L. A., Plasma in the Earth's polar magnetosphere, *J. Geophys. Res.*, **76**, 5203, 1971.
- Gosling, J. T., M. F. Thomsen, S. J. Bame, R. C. Elphic, and C. T. Russell, Observations of reconnection of interplanetary and lobe magnetic field lines at the high-latitude magnetopause, *J. Geophys. Res.*, **96**, 10,097, 1991.
- Gurnett, D. A., and R. R. Anderson, The kilometric radio emission spectrum: Relationship to auroral acceleration processes, in *Physics of Auroral Arc Formation*, *Geophys. Monogr. Ser.*, vol. 25, edited by S.-I. Akasofu and J. R. Kan, p. 341, AGU, Washington, D. C., 1981.
- Gurnett, D. A., and L. A. Frank, A region of intense plasma wave turbulences on auroral field lines, *J. Geophys. Res.*, **69**, 1031, 1977.
- Gurnett, D. A., and L. A. Frank, Plasma waves in the polar cusp: Observations from Hawkeye 1, *J. Geophys. Res.*, **83**, 1447, 1978.
- Haerendel, G., and G. Paschmann, Entry of solar wind plasma into the magnetosphere, in *Physics of the Hot Plasma in the Magnetosphere*, edited by B. Hultqvist and L. Stenflo, p. 23, Plenum, New York, 1975.
- Haerendel, G., G. Paschmann, N. Scopke, H. Rosenbauer, and R. C. Hedgecock, The frontside boundary layer of the magnetosphere and the problem of reconnection, *J. Geophys. Res.*, **83**, 3195, 1978.
- Heikkila, W. J., and J. D. Winningham, Penetration of magnetosheath plasma to low altitudes through the day side magnetospheric cusps, *J. Geophys. Res.*, **76**, 883, 1971.
- Kessel, R. L., S.-H. Chen, J. L. Green, S. F. Fung, S. A. Boardsen, L. C. Tan, T. E. Eastman, J. D. Craven, and L. A. Frank, Evidence of high-latitude reconnection during northward IMF: Hawkeye observations, *Geophys. Res. Lett.*, **23**, 583, 1996.
- Kivelson, M. G., C. T. Russell, M. Neugebauer, F. L. Scarf, and R. W. Fredricks, Dependence of the polar cusp on the north-south component of the interplanetary magnetic field, *J. Geophys. Res.*, **78**, 3761, 1973.
- Lemaire, J., and M. Roth, Penetration of solar wind plasma elements into the magnetosphere, *J. Atmos. Terr. Phys.*, **40**, 331, 1978.
- Lepping, R. P., and K. W. Behannon, Magnetic field directional discontinuities: I. Minimum variances errors, *J. Geophys. Res.*, **85**, 4695, 1980.
- McPherron, R. L., C. T. Russell, and P. J. Coleman Jr., Fluctuating magnetic fields in the magnetosphere, II, ULF waves, *Space Sci. Rev.*, **13**, 411, 1972.
- Meng, C.-I., Case studies of the storm time variation of the polar cusp, *J. Geophys. Res.*, **88**, 137, 1983.
- Paschmann, G., G. Haerendel, N. Scopke, H. Rosenbauer, and P. C. Hedgecock, Plasma and magnetic field characteristics of the distant polar cusp near local noon: The entry layer, *J. Geophys. Res.*, **81**, 2883, 1976.
- Paschmann, G., B. U. Ö. Sonnerup, I. Papamastorakis, N. Scopke, G. Haerendel, S. J. Bame, J. R. Asbridge, J. T. Gosling, C. T. Russell, and R. C. Elphic, Plasma acceleration at the Earth's magnetopause: Evidence for reconnection, *Nature*, **243**, 1979.
- Paschmann, G., B. U. Ö. Sonnerup, I. Papamastorakis, W. Baumjohann, N. Scopke, and H. Lühr, The magnetopause and boundary layer for small magnetic shear: Convection electric field and reconnection, *Geophys. Res. Lett.*, **17**, 18,239, 1990.
- Phillips, J. L., S. J. Bame, R. C. Elphic, J. T. Gosling, M. F. Thomsen,

- and T. G. Onsager, Well-resolved observations by ISEE 2 of ion dispersion in the magnetospheric cusp, *J. Geophys. Res.*, **98**, 13,429, 1993.
- Potemra, T. A., R. E. Erlandson, L. J. Zanetti, R. L. Arnoldy, J. Woch, and E. Friis-Christensen, The dynamic cusp, *J. Geophys. Res.*, **97**, 2835, 1992.
- Reiff, P. H., T. W. Hill, and J. L. Burch, Solar wind plasma injection at the dayside magnetospheric cusp, *J. Geophys. Res.*, **82**, 479, 1977.
- Reiff, P. H., J. L. Burch, and R. W. Spiro, Cusp proton signatures and the interplanetary magnetic field, *J. Geophys. Res.*, **85**, 5997, 1980.
- Rosenbauer, H., H. Grunwaldt, M. D. Montgomery, G. Paschmann, and N. Sckopke, Heos 2 plasma observations in the distant polar magnetosphere: The plasma mantle, *J. Geophys. Res.*, **80**, 2723, 1975.
- Russell, C. T., C. R. Chappell, M. D. Montgomery, M. Neugebauer, and F. L. Scarf, Heos 2 observations of the polar cusp on November 1, 1968, *J. Geophys. Res.*, **76**, 6743, 1971.
- Saflekos, N. A., T. A. Potemra, P. M. Kintner Jr., and J. L. Green, Field-aligned currents, convection electric fields, and ULF-ELF waves in the cusp, *J. Geophys. Res.*, **84**, 1391, 1979.
- Sandholt, P. E., A. Egeland, C. S. Deehr, G. G. Sivjee, and G. J. Romick, Effects of interplanetary magnetic field and magnetospheric substorm variations on the dayside aurora, *Planet. Space Sci.*, **31**, 1345, 1983.
- Scarf, F. L., R. W. Fredricks, I. M. Green, and C. T. Russell, Plasma waves in the dayside polar cusp: 1. Magnetospheric observations, *J. Geophys. Res.*, **77**, 2274, 1972.
- Scarf, F. L., R. W. Fredricks, M. Neugebauer, and C. T. Russell, Plasma waves in the dayside polar cusp, 2. Magnetopause and polar magnetosheath, *J. Geophys. Res.*, **79**, 511, 1974.
- Sibeck, D. G., R. E. Lopez, and E. C. Roelof, Solar wind control of the magnetopause shape, location and motion, *J. Geophys. Res.*, **96**, 5489, 1991.
- Siscoe, G. L., L. Davis Jr., P. J. Coleman Jr., E. J. Smith, and D. E. Jones, Power spectra and discontinuities of the interplanetary magnetic field: Marina 4, *J. Geophys. Res.*, **73**, 61–82, 1968.
- Sonnerup, B. U. Ö., Magnetopause reconnection rate, *J. Geophys. Res.*, **79**, 154, 1974.
- Sonnerup, B. U. Ö., and L. J. Cahill Jr., Magnetopause structure and attitude from Explorer 12 observations, *J. Geophys. Res.*, **72**, 171, 1967.
- Sonnerup, B. U. Ö., I. Papamastorakis, G. Paschmann, and H. Lüher, The magnetopause for large magnetic shear: Analysis of convection electric fields from AMPTE/IRM, *J. Geophys. Res.*, **95**, 10,541, 1990.
- Tsyganenko, N. A., A magnetospheric magnetic field model with a warped tail current sheet, *Planet. Space Sci.*, **37**, 5, 1989.
- Van Allen, J. A., and J. Adnan, Observed current on the Earth's high-latitude magnetopause, *J. Geophys. Res.*, **97**, 6381, 1992.
- Van Allen, J. A., M. N. Oliven, and R. A. Fliehler, Magnetic field in the Earth's polar magnetosphere to 21  $R_E$  (abstract), *Eos Trans. AGU*, **55**, 1167, 1974.
- Vasyliunas, V. M., The origin of the plasma sheet: Relevant observations and theoretical considerations, paper presented at Substorm Conference, Rice Univ., AGU, Houston, Tex., 1972.
- S. A. Boardsen, S.-H. Chen, and L. C. Tan, Hughes STX Corporation, Code 630, NASA/GSFC, Greenbelt, MD 20771. (e-mail: chen@bolero.gsfc.nasa.gov; boardsen@nssdca.gsfc.nasa.gov; ltan@nssdca.gsfc.nasa.gov)
- J. D. Craven, Geophysical Institute and Department of Physics, University of Alaska, Fairbanks, Alaska 99775-7320.
- T. E. Eastman, Institute for Physical Science and Technology, University of Maryland, College Park, MD 20742. (e-mail: eastman@ipst.umd.edu)
- S. F. Fung, J. L. Green, and R. L. Kessel, Code 630, NASA Goddard Space Flight Center, Greenbelt, MD 20771. (e-mail: fung@nssdca.gsfc.nasa.gov; green@nssdca.gsfc.nasa.gov; kessel@nssdca.gsfc.nasa.gov)

(Received June 27, 1996; revised March 3, 1997; accepted March 4, 1997.)